


Universality of phonon transport in nanowires dominated by surface roughness

P. Markoš

Department of Experimental Physics, Comenius University in Bratislava, 842 28 Bratislava, Slovakia

K. A. Muttalib

Department of Physics, University of Florida, Gainesville, Florida 32611-8440, USA (Received 26 November 2017; revised manuscript received 15 January 2018; published 16 February 2018)

We analyze, both theoretically and numerically, the temperature-dependent thermal conductivity κ of two-dimensional nanowires with surface roughness. Although each sample is characterized by three independent parameters, the diameter (width) of the wire, the correlation length, and the strength of the surface corrugation, our theory predicts that there exists a universal regime where κ is a function of a single combination of all three model parameters. Numerical simulations of propagation of acoustic phonons across thin wires confirm this universality and predict a $d^{1/2}$ dependence of κ on the diameter d .

DOI: [10.1103/PhysRevB.97.085423](https://doi.org/10.1103/PhysRevB.97.085423)**I. INTRODUCTION**

The challenge of designing a good thermoelectric device is, in part, to find a thermoelectric material that is simultaneously an “electron crystal and phonon glass” [1,2], i.e., a thermoelectric material with a large electrical but small thermal conductivity. This combination allows a large thermoelectric current without much heat dissipation, leading to high efficiency. Significant efforts have gone into the art of nanoengineering novel materials with such properties [3,4]. On the other hand, it has been proposed recently that a device consisting of a number of parallel nanowires with an external gate voltage can be used [5] to exploit the interplay of the material parameters with the thermodynamic parameters in the nonlinear transport regime, which can have both a large thermoelectric efficiency and a significant power output [6]. While the nanowires are not necessarily “phonon glasses,” strong *surface disorder* can suppress phonon transport significantly in Si nanowires with diameters $d < 100$ nm, as demonstrated in recent experiments [7–10]. This is particularly important in the context of thermoelectric devices since surface disorder is expected to suppress phonons more than electrons if the electron mean free path is much smaller than the diameter of the wire.

The effect of surface roughness on phonon transport in nanowires has been studied numerically using Monte Carlo [11,12] and molecular dynamics [13–16] simulations as well as models using the wave-scattering formalism [17–22]. These studies show that the thermal conductivity in such cases can be much smaller than when the surface scattering is fully diffusive. Other theoretical models have considered only diffusive boundary scattering, together with various scattering mechanisms within the bulk [23–26]. A recent work [27] has argued that the suppression of phonon transport in a surface-roughness-dominated nanowire can be understood within a simple theoretical model that incorporates scattering of propagating phonons off localized phonons, where the localized phonons appear as a result of an exact mapping [28] from a

model with surface disorder to a model with a smooth surface with additional channel-mixing pseudointeractions. The model with localized phonons has clear predictions about how the thermal conductivity depends on the various parameters that characterize the surface disorder, as well as on the parameters that characterize the localized phonons. However, these latter parameters are phenomenological and have not been obtained from any microscopic considerations.

As is clear from experiments [8–10], the effect of surface disorder depends crucially on the way the wire is prepared, using electroless etching (ELE) or vapor-liquid-solid (VLS) techniques. Evidently, nanowires prepared with ELE have thermal conductivity κ significantly smaller than those prepared with VLS. For VLS wires, as the diameter d is decreased, the low-temperature behavior of κ apparently changes from a T^3 dependence for $d = 115$ nm to a T^2 dependence for $d = 37$ nm [8]. The high-temperature behavior ($T > 100$ K) shows a downturn consistent with the importance of umklapp scattering in this regime. Theoretical models taking into account all significant bulk scattering mechanisms, changes in dispersion relations, and a diffusive boundary have been used to fit the experimental results for VLS wires [29]. In contrast, the ELE wires seem to be qualitatively different. The low- T behavior of ELE wires seems to follow a T^2 dependence for all $115 \leq d \leq 50$ nm, and the high- T behavior does not show any downturn up to $T = 300$ K. This suggests that the ELE wires might be in a regime where the surface disorder dominates over all other bulk scattering mechanisms.

In this paper we consider phonon propagation in thin two-dimensional nanowires with only surface disorder as a simple model for phonon transport in the surface-roughness-dominated regime. We first analyze the theoretical model of Ref. [27] based on the scattering of propagating phonons off localized phonons and obtain the thermal conductivity κ for wires of diameter (width) d for a fixed length $L \gg d$. The surface disorder is characterized by an rms height h of the roughness profile and a correlation length l_c . Although κ in general depends on all of the parameters d , h , and l_c , we show

analytically in the present work that there exists a *universal regime* where κ depends only on a single combination of all three parameters. This universal regime should be observable in all surface-roughness-dominated nanowires. While we show the existence of a single parameter by analyzing the simple model of Ref. [27], the actual dependence on all three parameters cannot be obtained analytically. We therefore perform numerical simulations on wires with appropriate surface disorder and obtain the scaling parameter by fitting to a universal curve of thermal conductivity as a function of temperature. We show that in this universal regime the low-temperature dependence of κ is T^2 , and the high-temperature behavior is independent of temperature. In addition, the diameter dependence of the thermal conductivity turns out to be approximately $d^{1/2}$. More generally, $\kappa(T)$ can be expressed in terms of a single parameter, $\zeta = \sqrt{l_c d}/h$, which is consistent with the experimental results of Ref. [10]. The universality holds only in the diffusive regime, characterized by a $1/L$ dependence of the thermal conductance on the length of the wire.

All of the above properties are consistent with the ELE wires and inconsistent with the VLS wires; we therefore conclude that the ELE wires are indeed in the surface-disorder-dominated regime. More importantly, the universal scaling predicts that there are different possibilities of combining the parameters d , h , and l_c to reach the same level of thermal conductivity, which might allow flexibility in designing a good thermoelectric device based on nanowires.

II. THEORETICAL MODEL

In the theoretical model of Ref. [27], the problem of phonons propagating in a disordered wire with surface roughness is mapped onto a problem of propagating phonons along a wire with a smooth surface and additional interaction with localized phonons, where the localized phonons have properties determined by the characteristics of the original model of surface disorder. We will consider a two-dimensional (2D) system, with length $L \gg d$. We characterize the surface disorder by a Lorentzian power spectrum

$$S(q; \Delta, l_c) = \frac{\Delta^2 l_c}{1 + q^2 l_c^2}, \quad \Delta \equiv \frac{h}{d}. \quad (1)$$

It then follows from Ref. [27] that the scattering rate of propagating phonons scattering off localized phonons in surface-roughness-dominated nanowires should depend on the combined roughness parameter

$$R_0 \equiv \frac{\Delta^2}{l_c}. \quad (2)$$

In addition, the existence of localized phonons suggests that the scattering rate should also depend on the parameters of the localized phonons, namely, the widths Γ_i and the frequencies Ω_i . For simplicity, we will assume a fixed boundary condition at the surface which will allow us to make a direct comparison with the numerical studies in Sec. III. While this will, in effect, leave out some of the low-frequency surface modes [22], we will argue later that the experiments with ELE wires are consistent with the absence (or very low density) of low-frequency localized phonons. Thus we expect the localized phonons to be a discreet set and to have typically high frequencies, of the

order of $\sqrt{k/M}$, where k is the spring constant associated with the atoms in the material and M is the typical cluster mass that takes part in the localized vibrations. Suppose the lowest frequency is Ω_1 . For simplicity we will also assume that for a given disorder, the widths of the relevant localized phonons are approximately the same, i.e., $\Gamma_i \approx \Gamma$. This is a reasonable approximation since the width largely depends on the effective barrier height and width that characterizes a given surface roughness. The contribution from the localized phonons to the scattering rate is roughly proportional to [27]

$$\begin{aligned} \frac{1}{2\tau(\omega)} &\propto R_0 \sum_i \Gamma_i \left[\frac{1}{(\omega - \Omega_i)^2 + \Gamma_i^2} - \frac{1}{(\omega + \Omega_i)^2 + \Gamma_i^2} \right] \\ &\approx R_0 \sum_i \frac{2\omega\Omega_i\Gamma}{[(\omega - \Omega_i)^2 + \Gamma^2][(\omega + \Omega_i)^2 + \Gamma^2]}. \end{aligned} \quad (3)$$

In the low-temperature regime almost all contributions to the thermal conductivity come from the low-frequency regime $\omega \ll \Omega_1$, where the scattering rate can be approximated as

$$\frac{1}{2\tau(\omega)} \rightarrow R_0 \frac{2\omega\Omega_1\Gamma}{[\Omega_1^2 + \Gamma^2]^2} \approx R_0 \frac{2\omega\Gamma}{\Omega_1^3}. \quad (4)$$

Here only the localized phonon with the lowest frequency contributes, and we have assumed $\Gamma \ll \Omega_1$.

In the opposite limit of large $\omega \geq \Omega_1$, the scattering rate will be dominated by the resonant scatterings from each localized phonon at $\omega = \Omega_i$. The total contribution from all the localized phonons will then be approximately

$$\frac{1}{2\tau(\omega)} \approx R_0 \sum_i \frac{1}{\Gamma_i} \approx R_0 \frac{n_{\text{loc}}}{\Gamma}, \quad (5)$$

where n_{loc} is the number of localized phonons within the propagating band. Thus the factor determining the disorder dependence of the scattering rate is expected to be

$$\begin{aligned} \frac{1}{2\tau(\omega)} &\propto \left(\frac{\Delta^2}{l_c} \right) \frac{\omega\Gamma}{\Omega_1^3}, \quad \omega \ll \Omega_1, \\ &\propto \left(\frac{\Delta^2}{l_c} \right) \frac{n_{\text{loc}}}{\Gamma}, \quad \omega \geq \Omega_1. \end{aligned} \quad (6)$$

The transmission function is proportional to the scattering time $\tau(\omega)$, the inverse of the scattering rate, multiplied by the propagating phonon velocities $v_L v_R = \omega^2(2\omega_0^2 - \omega^2)$ with the band edge at $\sqrt{2}\omega_0$. The thermal conductivity in the diffusive regime then can be written as

$$\kappa = \int_0^{\sqrt{2}\omega_0} d\omega \omega \tau(\omega) \omega^2(2\omega_0^2 - \omega^2) \frac{\partial \eta}{\partial T}, \quad (7)$$

where η is the Bose distribution function $\eta \equiv 1/(e^{\omega/T} - 1)$ and we have chosen the Boltzmann constant $k_B = 1$. The derivative has the limits

$$\begin{aligned} \frac{\partial \eta}{\partial T} &= \frac{\omega}{T^2} \frac{e^{\omega/T}}{(e^{\omega/T} - 1)^2} \approx \frac{\omega}{T^2} \frac{T^2}{\omega^2} \sim \frac{1}{\omega}, \quad \omega \ll T, \\ &\approx \frac{\omega}{T^2} e^{-\omega/T}, \quad \omega \gg T. \end{aligned} \quad (8)$$

A. Low-temperature regime

For $T < \Omega_1$, we can approximate the ω integral as follows:

$$\begin{aligned} \kappa \approx & \int_0^T d\omega \omega \tau(\omega) \omega^2 2\omega_0^2 \frac{1}{\omega} \\ & + \int_T^{\sqrt{2}\omega_0} d\omega \omega \tau(\omega) \omega^2 (2\omega_0^2 - \omega^2) \frac{\omega}{T^2} e^{-\omega/T}. \end{aligned} \quad (9)$$

The second integral can be neglected due to the exponential. Using the low-frequency expression for the scattering rate, we can then write

$$\begin{aligned} \kappa \propto & \frac{l_c}{\Delta^2} \frac{\Omega_1^3}{\Gamma} 2\omega_0^2 \int_0^T d\omega \omega \\ = & \frac{l_c}{\Delta^2} \frac{\Omega_1^3}{\Gamma} \omega_0^2 T^2, \quad T \ll \Omega_1. \end{aligned} \quad (10)$$

Thus the thermal conductivity has a T^2 dependence in the low-temperature regime for all values of the diameter and disorder parameters. This seems to be the case for all of the ELE wires in the regime $50 \leq d \leq 115$ nm but is not true for the VLS wires where the $d = 115$ nm wire has a T^3 dependence.

B. High-temperature regime

In the regime $T > \Omega_1$, the thermal conductivity can be approximated as

$$\begin{aligned} \kappa \approx & \int_0^{\Omega_1} d\omega \omega \tau(\omega) \omega^2 2\omega_0^2 \frac{1}{\omega} \\ & + \int_{\Omega_1}^T d\omega \omega \tau(\omega) \omega^2 (2\omega_0^2 - \omega^2) \frac{1}{\omega} \\ & + \int_T^{\sqrt{2}\omega_0} d\omega \omega \tau(\omega) \omega^2 (2\omega_0^2 - \omega^2) \frac{\omega}{T^2} e^{-\omega/T}. \end{aligned} \quad (11)$$

Again, we neglect the third integral due to the exponential term. The second term is proportional to $\frac{l_c}{\Delta^2} \frac{\Gamma}{n_{\text{loc}}} \int_{\Omega_1}^T d\omega \omega^2 (2\omega_0^2 - \omega^2)$. This is much smaller than the first term since $\Gamma \ll \Omega_1$, so κ is approximately given by the first term, which is independent of T ,

$$\kappa \propto \frac{l_c}{\Delta^2} \frac{\Omega_1^3}{\Gamma} \omega_0^2 \Omega_1^2, \quad T \gg \Omega_1. \quad (12)$$

Thus the thermal conductivity saturates in the high-temperature limit, with the saturation value depending on the roughness parameters as well as the diameter of the wire. The ELE wires show this saturation for $T > 200$ K, with the saturation value increasing with d . In contrast, the thermal conductivities of the VLS wires have maxima between 100 and 200 K and do not saturate for any of the diameters $115 \geq d \geq 37$ nm up to $T = 300$ K. We note that the crossover temperature Ω_1 is large for all of the ELE samples, which justifies our assumption of a fixed boundary condition. At the same time, the Van Hove singularity in 2D at ω_{VH} does not affect the thermal conductivity significantly if $\Omega_1 < \omega_{\text{VH}}$.

C. Conjecture for universality

We will assume that while the width of the localized phonons depends on the roughness parameters, the lowest

frequency Ω_1 does not. This is consistent with our initial assumption that the frequency is largely dictated by the mass of the atoms taking part in the localized vibrations. Then for the entire range of temperature, the thermal conductivity is proportional to the parameter

$$C(d, h, l_c) \equiv \left(\frac{l_c}{\Delta^2} \right) \frac{1}{\Gamma}. \quad (13)$$

It is not clear how to obtain the roughness parameter dependence of Γ , but we expect it to increase with increasing d and increasing l_c but decrease with increasing h . In the absence of a detailed microscopic theory, we propose the following as a conjecture:

$$\Gamma \propto \frac{d^\alpha l_c^\gamma}{h^\mu}, \quad (14)$$

where α , γ , and μ are all positive. Then

$$\kappa \propto C(d, h, l_c) \propto \frac{d^{2-\alpha} l_c^{1-\gamma}}{h^{2-\mu}}. \quad (15)$$

This suggests that for a given constant $C(d, h, l_c)$, all plots of thermal conductivity as a function of temperature for various choices of the parameters d , h , and l_c should fall on top of each other if the exponents α , γ , and μ are known. This universality is a feature of phonon transport only in the surface-roughness-dominated nanowires. Unfortunately, it is not possible to determine the exponents from the present theoretical model. In the following section we will test the conjecture of universality numerically and obtain the exponents $\alpha \approx 3/2$, $\gamma \approx 1/2$, and $\mu \approx 1$ for a two-dimensional wire. Thus the thermal conductivity will be shown to be a universal function of the single parameter

$$\zeta \equiv \frac{l_c^{1/2}}{h} d^{1/2}. \quad (16)$$

III. NUMERICAL SIMULATIONS

A. The model

We will compare (15) with numerical simulations. For simplicity, we will assume a fixed boundary condition at the surface which was also assumed in Sec. II. In addition we will consider only longitudinal phonons since, within our approximation, adding transverse phonons should not change either the temperature dependence or the eventual scaling properties of thermal conductivity. In our model, the sample is represented by a square lattice with lattice constant $a = 1$. For the atom located at site xy , the wave equation reads

$$\sqrt{\frac{m_{xy}}{k}} \omega^2 u_{xy} = u_{x+1y} + u_{x-1y} + u_{xy+1} + u_{xy-1}, \quad (17)$$

with the atomic mass $m_{xy} = m = 1$ and spring constant $k = 1$. The size of the lattice is $d \times L$. In numerical simulations, d increases from 64 to 256, and the length of the system was chosen to be $L > 1000$. This corresponds to nanowires with a width of 12–50 nm and length > 200 nm.

In order to create the surface disorder of the nanowire with appropriate h and l_c , we first generate a set of random numbers $\{\xi_x\}$, $x = 1, 2, \dots, L$, with zero mean and correlation $\langle \xi_x \xi_{x'} \rangle = h^2 \exp -|x - x'|/l_c$. Then we define a surface profile

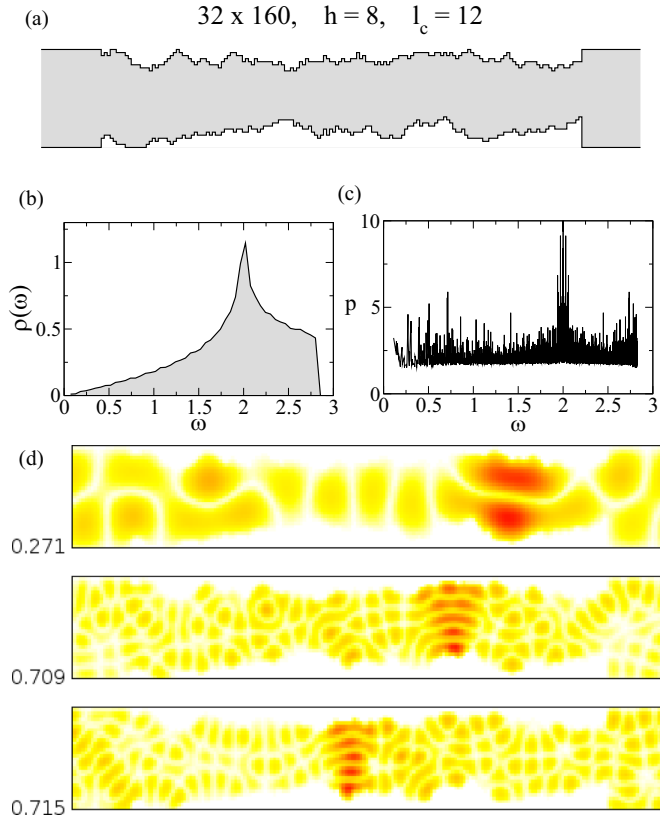


FIG. 1. (a) Typical sample under study. The disordered sample is attached to two semi-infinite leads. (b) Density of states $\rho(\omega)$ for a two-dimensional ideal square lattice. The bandwidth is $2\sqrt{2}$. Note the Van Hove singularity at $\omega = 2$. (c) Inverse participation ratio p as a function of frequency calculated for the sample in (a) with periodic boundary conditions in the horizontal direction. (d) Three localized phonons with eigenfrequencies $\omega = 0.27, 0.709$, and 0.719 . Shown is the absolute value $|u_n(\vec{r})|$. In red sites $|u_n(\vec{r})| > 0.05$ with a maximal value of 0.1 . White sites with zero phonon amplitude lie outside the wire.

$y_x = \xi_x + \delta$ with constant shift $\delta = -\min \xi_x$, which guarantees that $y_x \geq 0$ for each x . Then, for a given x , we substitute all atoms with $y \leq y_x$ by heavy atoms with mass $M = 10^4 m$. The opposite boundary of the sample is constructed in a similar way. This restricts phonons to propagate only in the region occupied by “light” atoms. The sample is attached to two semi-infinite ideal leads of width d . Figure 1(a) shows a typical sample.

Thanks to spatial periodicity of the lattice, the frequency spectrum in the leads consists of one frequency band, $0 \leq \omega \leq 2\sqrt{2}$ with the Van Hove singularity, typical for 2D systems, at $\omega = 2$. The phonon density of states is shown in Fig. 1(b).

To check the presence of localized states in the sample, we calculate all eigenfrequencies ω_n and (normalized) eigenfunctions $u_n(\vec{r})$ of the structure shown in Fig. 1(a). Localized states could be identified by analysis of the inverse participation ratio [30]

$$p_n = \frac{\sum_{\vec{r}} |u_n(\vec{r})|^4}{\sum_{\vec{r}} |u^{(0)}(\vec{r})|^4}, \quad (18)$$

where $u^{(0)}$ is any eigenfunction of the same system without surface disorder. The eigenstate is localized if $p_n \gg 1$. The plot

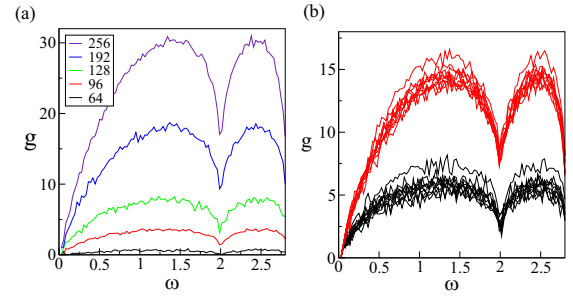


FIG. 2. (a) The ω dependence of g for samples of size $d \times 2048$, with $d = 64, 96, 128, 192$, and 256 . The surface roughness $h = 20$, and the correlation length $l_c = 100$. (b) $g(\omega)$ for ten samples with different realizations of surface disorder and size 128×2048 and correlation length $l_c = 200$. The surface disorder is $h = 17$ (top red curves) and $h = 29.5$ (bottom black curves).

of p as a function of frequency shown in Fig. 1(c) confirms that localized phonons exist mostly in the vicinity of the Van Hove singularity, and their density is low in the low-frequency part of the spectra. Three localized phonons are shown in Fig. 1(d).

B. Thermal conductance

We now use the standard Economou-Soukoulis formula [31]

$$g = \sum_i T_i \quad (19)$$

to obtain the transmission $g = g(\omega)$ as a function of frequency. In Eq. (19), $g(\omega)$ is given as a sum of contributions T_i of all open transmission channels. A detailed analysis shows that $g(\omega)$ typically consists of contribution from ballistic transmission channels with $T_i \approx 1$, diffusive channels, and some localized channels with negligible transmission T_i .

In numerical simulations, we map the wave model given by Eq. (17) into an electronic model

$$E\Phi_{xy} = \Phi_{x+1y} + \Phi_{x-1y} + \Phi_{xy+1} + \Phi_{xy-1} + V_{xy}\Phi_{xy}, \quad (20)$$

where energy $E = \omega^2$ and potential $V_{xy} = (m_{xy} - 1)\omega^2$. The method is described in Refs. [32,33].

Figure 2(a) shows a typical frequency dependence of the transmission $g(\omega)$. For low frequency, the transmission increases linearly as ω . The dip in the transmission at $\omega = 2$ corresponds to the Van Hove singularity in the density of states. Figure 2(b) proves, in agreement with previous numerical studies [34–36], that the value of the transmission depends on the realization of surface disorder. Observed transmission fluctuations are of order unity in the diffusive transport regime and increase when disorder increases.

Numerical data provide us with the transmission $g(\omega)$, which determines the thermal conductance K as

$$K = \int_0^{\omega_D} d\omega g(\omega) \left[\frac{\omega/2T}{\sinh(\omega/2T)} \right]^2. \quad (21)$$

The upper limit of the integration ω_D lies above the upper edge of the frequency band. The typical temperature dependence of

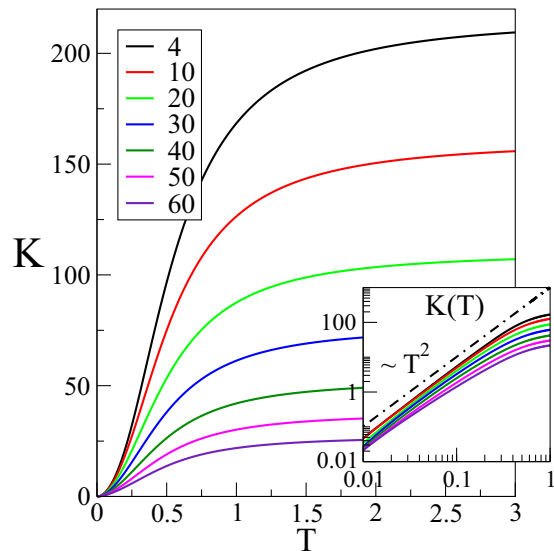


FIG. 3. Thermal conductance K given by Eq. (21) calculated numerically for sample size $d \times L = 256 \times 2048$. Correlation length $l_c = 400$. The surface roughness increases from $h = 4$ to $h = 60$. For all h , K exhibits the same T dependence. The inset shows $K(T) \sim T^2$ for small T . For large T , K saturates since our model does not include umklapp processes.

K is shown in Fig. 3, consistent with theoretical expectations of Eqs. (10) and (12).

Note that the thermal conductance does not coincide with the thermal conductivity discussed in the previous section. K depends on the geometrical size of the sample and is defined not only for the diffusive regime but also for ballistic and localized regimes. In the diffusive regime and two-dimensional geometry, the conductivity κ can be obtained as [37]

$$\kappa = K \frac{L}{d}. \quad (22)$$

Besides the phonon wavelength, our model introduces four length scales. The size of the sample is determined by its width d and length $L \gg d$. The disorder is given by the strength of the surface roughness h and correlation length l_c . Now we investigate how the thermal conductance depends on all of these parameters.

C. Universality

To compare the thermal conductance for different samples, we introduce an integral

$$I = \int_0^{T_{\max}} dT K(T), \quad (23)$$

with the upper limit $T_{\max} = 3$, and calculate how I depends on the model parameters. Owing to similar monotonic T dependence of $K(T)$ (Fig. 3), we expect that universality of I guarantees the universality of $K(T)$ for any value of T . As an example, we show in the inset of Fig. 4 the universality of conductance $K(T)$ for similar values of I . Furthermore, combining Eqs. (21) and (23) guarantees the universality of $g(\omega)$ for each frequency ω .

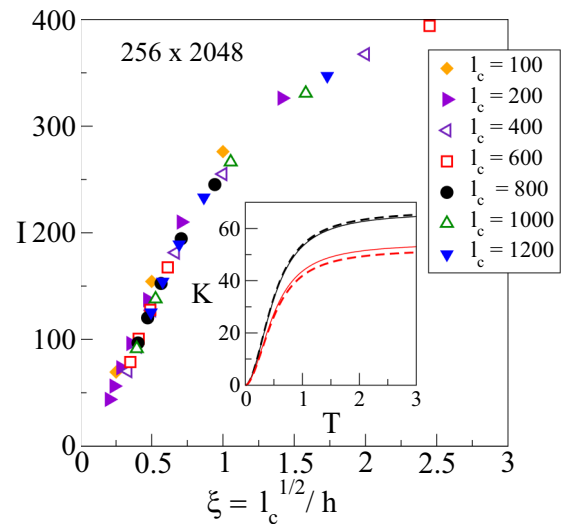


FIG. 4. Integral I , given by Eq. (23) for samples of size 256×2048 and various values of h and l_c . Data prove that for a given size of the system, I is a function of only one parameter, $\xi = \sqrt{l_c}/h$. The inset shows the universality of the function $K(T)$ for samples with the same value of integral I . Black lines show $l_c = 1200$, $h = 60$ ($I = 154$) and $l_c = 800$, $h = 50$ ($I = 152.5$). The small deviation between two displayed curves is given by different values of ξ . Red lines show $K(T)$ for two samples with $l_c = 1200$, $h = 70$ ($I = 125$) and $l_c = 800$, $h = 60$ ($I = 120.3$).

We find numerically that for a given system width d , I depends only on the combination

$$\xi = \frac{\sqrt{l_c}}{h}. \quad (24)$$

As an example, we show in Fig. 4 the integral I for system size $d \times L = 256 \times 2048$. Although the correlation length l_c increases by an order of magnitude from 100 to 1200 and disorder h varies between 4 and 70, all data collapse on a single curve. Similar universal $\sqrt{l_c}/h$ dependence was obtained for other widths of the sample (not shown).

The inset of Fig. 4 confirms our assumption, namely, that two samples with the same value of integral I possess the same T dependence of the thermal conductance $K(T)$.

Combining the results for different d , in Fig. 5 we plot I as a function of the parameter $z = d^{3/2}\xi = d^{3/2}l_c^{1/2}/h$. The interval of z in which $I(z) \propto z$ corresponds to the diffusive regime. As shown in Fig. 5, the slope of this linear dependence is universal. Using Eq. (22), the thermal conductivity κ then has universal dependence on the parameter $zL/d = \zeta L$, where ζ is given in Eq. (16). For larger values of z , the system is in the ballistic transmission regime, and the universality is lost. Similarly, for very small z we expect to reach a nonuniversal localized regime.

To prove that the universal linear dependence $I(\xi) \propto \xi$ corresponds to diffusive transport, we show in Fig. 6 the length dependence of I for various values of d and ξ . In the diffusive regime we find $I(\xi, L) \sim \xi/L$. For instance, in Fig. 6(a) the slope increases from 49 for $\xi = 0.5$ to 101 for $\xi = 1$. In Fig. 6(b) the slope increases from 75 to 126 when ξ increases from $2/3$ to 1. Similarly, Figs. 6(b) and 6(c)

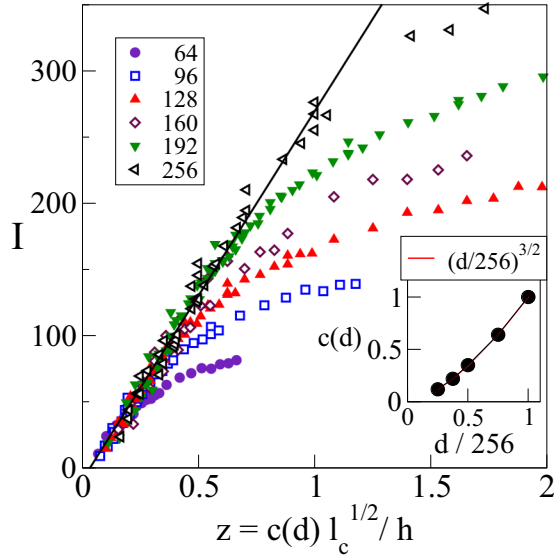


FIG. 5. Integral $I(l_c, h, d)$ for six widths of the system (given in the legend) as a function of parameter $z = d^{3/2} l_c^{1/2} / h$. The length of all systems is $L = 2048$. The solid line is a linear fit for $d = 256$ for data $I < 300$. The function $c(d) \propto d^{3/2}$ (shown in the inset) has been found to guarantee the overlap of data for all d in the linear (diffusive) regime $I(z) \propto z$.

confirm that samples with the same value of ξ possess the same slope (within the accuracy of numerical data). Finally, obtained values of the slope agree, at least qualitatively, with the predicted $d^{3/2}$ dependence on the width of the sample. For example, comparing $I(d_1 = 96)$ at $\xi = 1/2$ [solid triangles in Fig. 6(a)] with $I(d_2 = 256)$ for the same $\xi = 1/2$ [open triangles in Fig. 6(c)] at a fixed length, e.g., $1024/L = 0.25$, one can check that $I(d_1)/I(d_2) \approx 20/80 = 0.25$ agrees with $(d_1/d_2)^{3/2} = 0.23$ within the numerical accuracy.

To summarize, we conclude that the diffusive phonon transport is universal and

$$I \propto \sqrt{\frac{l_c}{d}} \frac{d}{h} \propto d^{3/2}. \quad (25)$$

This result differs from the diffusive regime in 2D samples with bulk disorder, where the conductance g is given by the equation [37]

$$g = \frac{\ell N}{L}. \quad (26)$$

Here ℓ is a mean free path of coherent scattering, and $N \propto d$ is the number of open channels. Thus we expect that for bulk disorder, $I \propto d$, in contrast to the $I \sim d^{3/2}$ dependence for samples with surface disorder. It should be emphasized that the $d^{3/2}$ dependence of the thermal conductance K corresponds to a $d^{1/2}$ dependence of the thermal conductivity κ , which depends on the single parameter ζ . We note that our result can be expressed in terms of an effective mean-free path that depends not only on the geometric parameter [38] d but also on the surface disorder parameters [20,39] l_c and h . We emphasize that our model is valid only in the surface-roughness-dominated regime.

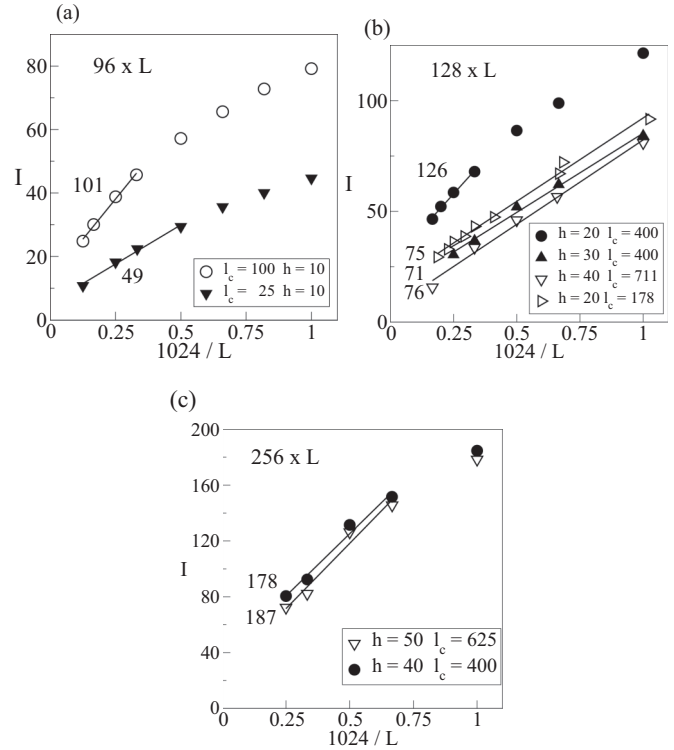


FIG. 6. The length dependence of the conductivity for various values of ξ and three widths of the samples, (a) $d = 96$, (b) 128 , and (c) 256 . Note that the slope of the linear width (given in the legend) is proportional to $\xi = \sqrt{l_c}/h$.

IV. DISCUSSION AND SUMMARY

In our numerical simulations we considered transmission of phonons across wires with surface corrugation. On the other hand, our theoretical model has localized phonons, characterized by phenomenological parameters, that arise from a mapping of the surface-disordered wire to a smooth wire with additional pseudointeractions [27]. It is therefore not clear how the phenomenological parameters of the localized phonons are related to the parameters characterizing the surface roughness. We can think of the localized phonon modes as corresponding to the resonances created inside the corrugations in our numerical simulations. In Eq. (15), we used qualitative arguments to argue that Γ must increase with increasing l_c and d but decrease with increasing h . Our numerical simulation suggests that Γ could be related to a simple power-law combination of all the parameters h, l_c , and d , given by $\Gamma \propto l_c^{1/2} d^{3/2} / h$, consistent with the above expectations. This immediately predicts a $d^{3/2}$ dependence of the thermal conductance and therefore a $d^{1/2}$ dependence of $\kappa(T)$. We note that the parameters h and l_c appear in the roughness power spectrum in the combination $l_c^{1/2}/h$, which is also the same combination that appears in Γ and therefore in the final result for $\kappa(T)$.

The breakdown of universality is clearly seen in Fig. 5 for either large l_c or small h , with both cases leading to a ballistic regime. The small- (d/h) regime, on the other hand, corresponds to the localized regime where the universality also fails. While theory calculates thermal conductivity, numerical

simulations obtain thermal conductance as a function of length L . In general, there is a nonuniversal part independent of L coming from, e.g., the contact resistance, and the universality holds only when the nonuniversal part is small compared to the diffusive part. As our results show, the diffusive regime, with a clear $1/L$ dependence of the thermal conductance, follows the universal behavior.

As predicted theoretically and confirmed numerically, the final result for κ as a function of T shows that in the surface-roughness-dominated regime, the low- T behavior is always T^2 , and the high- T behavior is independent of T . Both of these are clearly violated in the case of the VLS wires [8]. On the other hand, for the ELE wires the high- T behavior is clearly satisfied as noted before, and the low- T behavior is consistent with figures in Ref. [9]. The prediction of the $d^{1/2}$ behavior is clearly violated in the case of VLS wires with diameters $d = 37, 56, \text{ and } 115$ nm, while it is again consistent with figures in Ref. [9] with a similar range of diameters, $d = 50, 98, \text{ and } 115$ nm. Figure 3(a) of Ref. [10], with three different values of the three parameters $[(h, l_c, d; \zeta) = (4.3, 8.4, 69.7 \text{ nm}; 5.6),$

$(2.7, 8.4, 79.8 \text{ nm}; 9.6), \text{ and } (2.3, 8.9, 77.5 \text{ nm}; 11.4),$ all of which seem to be in the surface-disorder-dominated regime], is consistent with the single-parameter description of our model. Thus we argue that while the VLS wires are in the bulk-disorder-dominated regime, the ELE wires are in the surface-roughness-dominated regime. This then implies that similarly produced ELE wires should follow the universal one-parameter behavior, allowing flexibility in the choice of the various geometrical and disorder parameters to keep κ fixed at a low value.

ACKNOWLEDGMENTS

We acknowledge financial support from the Slovak Research and Development Agency under Contract No. APVV-15-0496 and from the agency VEGA under Contract No. 1/0108/17. K.A.M. thanks the Department of Experimental Physics, Faculty of Mathematics, Physics and Informatics at Comenius University for kind hospitality during his visit in fall 2017, when this work was partially carried out.

-
- [1] G. A. Slack, in *CRC Handbook of Thermoelectrics*, edited by D. M. Rowe (CRC Press, Boca Raton, FL, 1995), p. 407.
 - [2] G. J. Snyder and E. S. Toberer, *Nat. Mater.* **7**, 105 (2008).
 - [3] Y. Dubi and M. Di Ventra, *Rev. Mod. Phys.* **83**, 131 (2011).
 - [4] T. Takabatake, K. Suekuni, T. Nakayama, and E. Kaneshita, *Rev. Mod. Phys.* **86**, 669 (2014).
 - [5] K. A. Muttalib and S. Hershfield, *Phys. Rev. Appl.* **3**, 054003 (2015).
 - [6] S. Hershfield, K. A. Muttalib, and B. J. Nartowt, *Phys. Rev. B* **88**, 085426 (2013).
 - [7] A. I. Boukai, Y. Bunimovich, J. Tahir-Kheli, J.-K. Yu, W. A. Goddard III, and J. R. Heath, *Nature (London)* **451**, 168 (2008).
 - [8] D. Li, Y. Wu, P. Kim, L. Shi, P. Yang, and A. Majumdar, *Appl. Phys. Lett.* **83**, 2934 (2003).
 - [9] A. I. Hochbaum, R. Chen, R. D. Delgado, W. Liang, E. C. Garnett, M. Najarian, A. Majumdar, and P. Yang, *Nature (London)* **451**, 163 (2008).
 - [10] J. Lim, K. Hippalgaonkar, S. C. Andrews, A. Majumdar, and P. Yang, *Nano Lett.* **12**, 2475 (2012).
 - [11] A. L. Moore, S. K. Saha, R. S. Prasher, and L. Shi, *Appl. Phys. Lett.* **93**, 083112 (2008).
 - [12] D. Lacroix, *Appl. Phys. Lett.* **89**, 103104 (2006).
 - [13] D. Donadio and G. Galli, *Phys. Rev. Lett.* **102**, 195901 (2009).
 - [14] Y. He and G. Galli, *Phys. Rev. Lett.* **108**, 215901 (2012).
 - [15] T. Zushi, K. Ohmori, K. Yamada, and T. Watanabe, *Phys. Rev. B* **91**, 115308 (2015).
 - [16] L. Liu and X. Chen, *J. Appl. Phys.* **107**, 033501 (2010).
 - [17] D. H. Santamore and M. C. Cross, *Phys. Rev. B* **63**, 184306 (2001).
 - [18] D. H. Santamore and M. C. Cross, *Phys. Rev. Lett.* **87**, 115502 (2001).
 - [19] G. B. Akguc and J. Gong, *Phys. Rev. B* **80**, 195408 (2009).
 - [20] J. H. Oh, M. Shin, and M.-G. Jang, *J. Appl. Phys.* **111**, 044304 (2012).
 - [21] A. A. Maznev, *Phys. Rev. B* **91**, 134306 (2015).
 - [22] L. N. Maurer, S. Mei, and I. Knezevic, *Phys. Rev. B* **94**, 045312 (2016).
 - [23] B. A. Glavin, *Phys. Rev. Lett.* **86**, 4318 (2001).
 - [24] N. Mingo, *Phys. Rev. B* **68**, 113308 (2003).
 - [25] S. G. Walkauskas, D. A. Brodio, K. Kempa, and T. L. Reinecke, *J. Appl. Phys.* **85**, 2579 (1999).
 - [26] D. L. Nika, A. I. Cocemasov, C. I. Isacova, A. A. Balandin, V. M. Fomin, and O. G. Schmidt, *Phys. Rev. B* **85**, 205439 (2012).
 - [27] K. A. Muttalib and S. Abhinav, *Phys. Rev. B* **96**, 075403 (2017).
 - [28] Z. Tešanović, M. V. Jarić, and S. Maekawa, *Phys. Rev. Lett.* **57**, 2760 (1986).
 - [29] N. Mingo, L. Yang, D. Li, and A. Majumdar, *Nano Lett.* **3**, 1713 (2003).
 - [30] B. Kramer and A. MacKinnon, *Rep. Prog. Phys.* **56**, 1469 (1993).
 - [31] E. N. Economou and C. M. Soukoulis, *Phys. Rev. Lett.* **46**, 618 (1981).
 - [32] C. M. Soukoulis, E. N. Economou, G. S. Grest, and M. H. Cohen, *Phys. Rev. Lett.* **62**, 575 (1989).
 - [33] P. Markoš and C. M. Soukoulis, *Phys. Rev. B* **71**, 054201 (2005).
 - [34] A. García-Martín, J. A. Torres, J. J. Sáenz, and M. Nieto-Vesperinas, *Phys. Rev. Lett.* **80**, 4165 (1998).
 - [35] A. García-Martín, T. López-Cuiudad, J. J. Sáenz, and M. Nieto-Vesperinas, *Phys. Rev. Lett.* **81**, 329 (1998).
 - [36] J. Feilhauer and M. Moško, *Phys. Rev. B* **83**, 245328 (2011).
 - [37] J.-L. Pichard, in *Quantum Coherence in Mesoscopic Systems*, edited by B. Kramer, NATO ASI Series, Series B: Physics Vol. 254 (Plenum, New York, 1991), p. 369.
 - [38] N. Chernov, *J. Stat. Phys.* **88**, 1 (1997).
 - [39] L. N. Maurer, Z. Aksamija, E. B. Ramayya, A. H. Davoody, and I. Knezevic, *Appl. Phys. Lett.* **106**, 133108 (2015).